

Temperature Dependence of the Spin Resistivity in Ferromagnetic Thin Films

K. Akabli and H. T. Diep*

*Laboratoire de Physique Théorique et Modélisation, CNRS-Université de Cergy-Pontoise, UMR 8089
2, Avenue Adolphe Chauvin, 95302 Cergy-Pontoise Cedex, France*

The magnetic phase transition is experimentally known to give rise to an anomalous temperature-dependence of the electron resistivity in ferromagnetic crystals. Phenomenological theories based on the interaction between itinerant electron spins and lattice spins have been suggested to explain these observations. In this paper, we show by extensive Monte Carlo (MC) simulation the behavior of the resistivity of the spin current calculated as a function of temperature (T) from low- T ordered phase to high- T paramagnetic phase in a ferromagnetic film. We analyze in particular effects of film thickness, surface interactions and different kinds of impurities on the spin resistivity across the critical region. The origin of the resistivity peak near the phase transition is shown to stem from the existence of magnetic domains in the critical region. We also formulate in this paper a theory based on the Boltzmann's equation in the relaxation-time approximation. This equation can be solved using numerical data obtained by our simulations. We show that our theory is in a good agreement with our MC results. Comparison with experiments is discussed.

PACS numbers: 72.25.-b ; 75.47.-m

I. INTRODUCTION

The electric resistivity in magnetic metals has been studied for years. The main effect of spin-independent resistivity is unanimously attributed to phonons. As far as spin-dependent resistivity is concerned, we had to wait until de Gennes and Friedel's first explanation in 1958¹ which was based on the interaction between spins of conduction electrons and magnetic lattice ions. Experiments have shown that the resistivity indeed depends on the spin orientation.^{2,3,4,5,6} Therefore, the resistivity was expected to depend strongly on the spin ordering of the system. Experiments on various magnetic materials have found in particular an anomalous behavior of the resistivity at the critical temperature where the system undergoes the ferromagnetic-paramagnetic phase transition.^{3,4,5,6} The problem of spin-dependent transport has been also extensively studied in magnetic thin films and multilayers. The so-called giant magnetoresistance (GMR) was discovered experimentally twenty years ago.^{7,8} Since then, intensive investigations, both experimentally and theoretically, have been carried out.^{9,10} The so-called "spintronics" was born with spectacular rapid developments in relation with industrial applications. For recent overviews, the reader is referred to Refs. 11 and 12. Theoretically, in their pioneer work, de Gennes and Friedel¹ have suggested that the magnetic resistivity is proportional to the spin-spin correlation. In other words, the spin resistivity should behave as the magnetic susceptibility. This explained that the resistivity singularity is due to "long-range" fluctuations of the magnetization observed in the critical region. Craig et al¹³ in 1967 and Fisher and Langer¹⁴ in 1968 criticized this explanation and suggested that the shape of

the singularity results mainly from "short-range" interaction at $T \gtrsim T_c$ where T_c is the transition temperature of the magnetic crystal. Fisher and Langer have shown in particular that the form of the resistivity cusp depends on the interaction range. An interesting summary was published in 1975 by Alexander and coworkers¹⁵ which highlighted the controversial issue. To see more details on the magnetic resistivity, we quote an interesting recent publication from Kataoka.¹⁶ He calculated the spin-spin correlation function using the mean-field approximation and he could analyze the effects of magnetic-field, density of conduction electron, the interaction range, etc. Although many theoretical investigations have been carried out, to date very few Monte Carlo (MC) simulations have been performed regarding the temperature dependence of the dynamics of spins participating in the current. In a recent work,¹⁷ we have investigated by MC simulations the effects of magnetic ordering on the spin current in magnetic multilayers. Our results are in qualitative agreement with measurements.¹⁸

Due to a large number of parameters which play certainly important roles at various degrees in the behavior of the spin resistivity, it is difficult to treat all parameters at the same time. The first question is of course whether the explanation provided by de Gennes and Friedel can be used in some kinds of material and that by Fisher and Langer can be applied in some other kinds of material. In other words, we would like to know the validity of each of these two arguments. We will return to this point in subsection III D. The second question concerns the effects of magnetic or non-magnetic impurities on the resistivity. Note that in 1970, Shwerner and Cuddy³ have shown and compared their experimental results with the different existing theories to understand the impurity effect on the magnetic resistivity. However, the interpretation was not clear enough at the time to understand the real physical mechanism lying behind. The third question concerns the effects of the surface on the spin resistivity

*Corresponding author, E-mail: diep@u-cergy.fr

in thin films. These questions have motivated the present work.

In this paper we use extensive MC simulation to study the transport of itinerant electrons traveling in a ferromagnetic thin film. We use the Ising model and take into account various interactions between lattice spins and itinerant spins. We show that the magnetic resistivity depends on the lattice magnetic ordering. We analyze this behavior by using a new idea: instead of calculating the spin-spin correlation, we calculate the distribution of clusters in the critical region. We show that the resistivity depends on the number and the size of clusters of opposite spins. We establish also a Boltzmann's equation which can be solved using numerical data for the cluster distribution obtained by our MC simulation.

The paper is organized as follows. Section II is devoted to the description of our model and the rules that govern its dynamics. We take into account (i) interactions between itinerant and lattice spins, (ii) interactions between itinerant spins themselves and (iii) interactions between lattice spins. We include a thermodynamic force due to the gradient of itinerant electron concentration, an applied electric field and the effect of a magnetic field. For impurities, we take the Rudermann-Kittel-Kasuya-Yoshida (RKKY) interaction between them. In section III, we describe our MC method and discuss the results we obtained. We develop in section IV a semi-numerical theory based on the Boltzmann's equation. Using the results obtained with Hoshen and Kopelman's¹⁹ cluster-counting algorithm, we show an excellent agreement between our theory and our MC data. Concluding remarks are given in Section V.

II. INTERACTIONS AND DYNAMICS

A. Interactions

We consider in this paper a ferromagnetic thin film. We use the Ising model and the face-centered cubic (FCC) lattice with size $4N_x \times N_y \times N_z$. Periodic boundary conditions (PBC) are used in the xy planes. Spins localized at FCC lattice sites are called "lattice spins" hereafter. They interact with each other through the following Hamiltonian

$$\mathcal{H}_l = -J \sum_{\langle i,j \rangle} \mathbf{S}_i \cdot \mathbf{S}_j, \quad (1)$$

where \mathbf{S}_i is the Ising spin at lattice site i , $\sum_{\langle i,j \rangle}$ indicates the sum over every nearest-neighbor (NN) spin pair $(\mathbf{S}_i, \mathbf{S}_j)$, $J(> 0)$ being the NN interaction.

In order to study the spin transport in the above system, we consider a flow of itinerant spins interacting with each other and with the lattice spins. The interaction between itinerant spins is defined as follows,

$$\mathcal{H}_m = - \sum_{\langle i,j \rangle} K_{i,j} \mathbf{s}_i \cdot \mathbf{s}_j, \quad (2)$$

where \mathbf{s}_i is the itinerant Ising spin at position \vec{r}_i , and $\sum_{\langle i,j \rangle}$ denotes a sum over every spin pair $(\mathbf{s}_i, \mathbf{s}_j)$. The interaction $K_{i,j}$ depends on the distance between the two spins, i.e. $r_{ij} = |\vec{r}_i - \vec{r}_j|$. A specific form of $K_{i,j}$ will be chosen below. The interaction between itinerant spins and lattice spins is given by

$$\mathcal{H}_r = - \sum_{\langle i,j \rangle} I_{i,j} \mathbf{s}_i \cdot \mathbf{S}_j, \quad (3)$$

where the interaction $I_{i,j}$ depends on the distance between the itinerant spin \mathbf{s}_i and the lattice spin \mathbf{S}_i . For the sake of simplicity, we assume the same form for $K_{i,j}$ and $I_{i,j}$, namely,

$$K_{i,j} = K_0 \exp(-r_{ij}) \quad (4)$$

$$I_{i,j} = I_0 \exp(-r_{ij}) \quad (5)$$

where K_0 and I_0 are constants.

B. Dynamics

The procedure used in our simulation is described as follows. First we study the thermodynamic properties of the film alone, i.e. without itinerant spins, using Eq. (1). We perform MC simulations to determine quantities as the internal energy, the specific heat, layer magnetizations, the susceptibility, ... as functions of temperature T .²⁰ From these physical quantities we determine the critical temperature T_c below which the system is in the ordered phase. We show in Fig. 1 the lattice magnetization versus T for $N_z = 8$, $N_x = N_y = 20$.

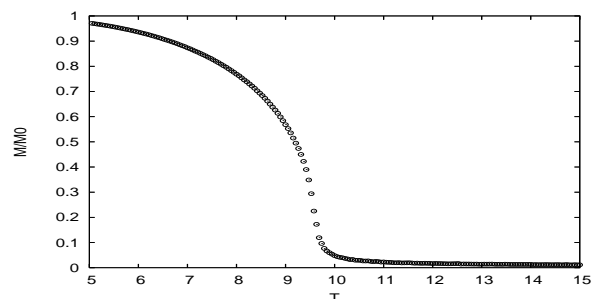


FIG. 1: Lattice magnetization versus temperature T for $N_z = 8$. T_c is $\simeq 9.58$ in unit of $J = 1$.

Once the lattice has been equilibrated at T , we inject N_0 itinerant spins into the system. The itinerant spins move into the system at one end, travel in the x direction, escape the system at the other end to reenter again at the first end under the PBC. Note that the PBC are used to

ensure that the average density of itinerant spins remains constant with evolving time (stationary regime). The dynamics of itinerant spins is governed by the following interactions:

i) an electric field \mathbf{E} is applied in the x direction. Its energy is given by

$$\mathcal{H}_E = -e\mathbf{E} \cdot \mathbf{v}, \quad (6)$$

where \mathbf{v} is the velocity of the itinerant spin, e its charge;

ii) a chemical potential term which depends on the concentration of itinerant spins ("concentration gradient" effect). Its form is given by

$$\mathcal{H}_c = Dn(\mathbf{r}), \quad (7)$$

where $n(\mathbf{r})$ is the concentration of itinerant spins in a sphere of radius D_2 centered at \mathbf{r} . D is a constant taken equal to K_0 for simplicity;

iii) interactions between a given itinerant spin and lattice spins inside a sphere of radius D_1 (Eq. 3);

iv) interactions between a given itinerant spin and other itinerant spins inside a sphere of radius D_2 (Eq. 2).

Let us consider the case without an applied magnetic field. The simulation is carried out as follows: at a given T we calculate the energy of an itinerant spin by taking into account all the interactions described above. Then we tentatively move the spin under consideration to a new position with a step of length v_0 in an arbitrary direction. Note that this move is immediately rejected if the new position is inside a sphere of radius r_0 centered at a lattice spin or an itinerant spin. This excluded space emulates the Pauli exclusion principle in the one hand, and the interaction with lattice phonons on the other hand. If the new position does not lie in a forbidden region of space, then the move is accepted with a probability given by the standard Metropolis algorithm.²⁰

To study the case with impurities, we replace randomly a number of lattice spins S by impurity spins σ . The impurities interact with each other via the RKKY interaction as follows

$$\mathcal{H}_I = - \sum_{\langle i,j \rangle} L(r_i, r_j) \sigma_i \cdot \sigma_j \quad (8)$$

where

$$L(r_i, r_j) = L_0 \cos(2k_F|r_i - r_j|)/|r_i - r_j|^3 \quad (9)$$

L_0 being a constant and k_F the Fermi wave number of the lattice. The impurity spins also interact with NN lattice spins. However, to reduce the number of parameters, we take this interaction equal to $J = 1$ as that between NN lattice spins (see Eq. 1) with however $\sigma \neq S$. We will consider two cases $\sigma = 2$ and $\sigma = 0$ in this paper.

III. MONTE CARLO RESULTS

We let N_0 itinerant spins travel through the system several thousands times until a steady state is reached.

The parameters we use in most calculations, except otherwise stated (for example, in subsection III B for N_z) are $s = S = 1$ and $N_x = N_y = 20$ and $N_z = 8$. Other parameters are $D_1 = D_2 = 1$ (in unit of the FCC cell length), $K_0 = I_0 = 2$, $L_0 = 17$, $N_0 = 8 \times 20^2$ (namely one itinerant spin per FCC unit cell), $v_0 = 1$, $k_F = (\frac{\pi}{a})(\frac{n_0}{2})^{1/3}$, $r_0 = 0.05$. At each T the equilibration time for the lattice spins lies around 10^6 MC steps per spin and we compute statistical averages over 10^6 MC steps per spin. Taking $J = 1$, we find that $T_c \simeq 9.58$ for the critical temperature of the lattice spins (see Fig. 1).

We define the resistivity ρ as

$$\rho = \frac{1}{n}, \quad (10)$$

where n is the number of itinerant spins crossing a unit area perpendicular to the x direction per unit of time.

A. Effect of thickness and effect of magnetic field.

We show in Figs. 2 and 3 the simulation results for different thicknesses. In all cases, the resistivity ρ is very small at low T , undergoes a huge peak in the ferromagnetic-paramagnetic transition region, decreases slowly at high T .

We point out that the peak position of the resistivity follows the variation of critical temperature with changing thickness (see Fig. 2) and ρ at $T \gtrsim T_c$ becomes larger when the thickness decreases. This is due to the fact that surface effects tend to slow down itinerant spins. We return to this point in the next subsection.

The temperature of resistivity's peak at a given thickness is always slightly higher than the corresponding T_c .

Let us discuss the temperature dependence of ρ shown in Fig. 3:

i) First, ρ is very low in the ordered phase. We can explain this by the following argument: below the transition temperature, there exists a single large cluster of lattice spins with some isolated "defects" (i. e. clusters of antiparallel spins), so that any itinerant spin having the parallel orientation goes through the lattice without hindrance. The resistance is thus very small but it increases as the number and the size of "defect" clusters increase with increasing temperature.

ii) Second, ρ exhibits a cusp at the transition temperature. We present here three interpretations of the existence of this cusp. Note that these different pictures are not contradictory with each other. They are just three different manners to express the same physical mechanism. The first picture consists in saying that the cusp is due to the critical fluctuations in the phase transition region. We know from the theory of critical phenomena that there is a critical region around the transition temperature T_c . In this region, the mean-field theory should take into account critical fluctuations. The width of this region is given by the Ginzburg criterion. The

limit of this "Ginzburg" region could tally with the resistivity's peak and Ginzburg temperature.¹⁵ The second picture is due to Fisher-Langer¹⁴ and Kataoka¹⁶ who suggested that the form of peak is due mainly to short-range spin-spin correlation. These short-range fluctuations are known to exist in the critical region around the critical point. The third picture comes from our MC simulation¹⁷ which showed that the resistivity's peak is due to the formation of antiparallel-spin clusters of sizes of a few lattice cells which are known to exist when one enters the critical region. Note in addition that the cluster size is now comparable with the radius D_1 of the interaction sphere, which in turn reduces the height of potential energy barriers. We have checked this interpretation by first creating an artificial structure of alternate clusters of opposite spins and then injecting itinerant spins into the system. We observed that itinerant spins do advance indeed more slowly than in the completely disordered phase (high- T paramagnetic phase). We have next calculated directly the cluster-size distribution as a function of T using the Hoshen-Kopelman's algorithm.¹⁹ The result confirms the effect of clusters on the spin conductivity. The reader is referred to our previous work¹⁷ for results of a multilayer case. We will show in the next section a cluster distribution for the film studied in this paper.

iii) Third, ρ is large in the paramagnetic phase and decreases with an increasing temperature. Above T_c in the paramagnetic phase, the spins become more disordered as T increases: small clusters will be broken into single disordered spins, so that there is no more energy barrier between successive positions of itinerant spins on their trajectory. The resistance, though high, is decreasing with increasing T and saturated as $T \rightarrow \infty$.

iv) Let us touch upon the effects of varying D_1 and D_2 at a low temperatures. ρ is very small at small D_1 ($D_1 < 0.8$): this can be explained by the fact that for such small D_1 , itinerant spins do not "see" lattice spins in their interaction sphere so they move almost in an empty space. The effect of D_2 is on the other hand qualitatively very different from that of D_1 : ρ is very small at small D_2 but it increases to very high value at large D_2 . We conclude that both D_1 and D_2 dominate ρ at their small values. However, at large values, only D_2 has a strong effect on ρ . This effect comes naturally from the criterion on the itinerant spins concentration used in the moving procedure. Also, we have studied the effect of the electric field E both above and below T_c . The low-field spin current verifies the Ohm regime. These effects have been also observed in magnetic multilayer.¹⁷ The reader is referred to that work for a detailed presentation of these points.

Let us show now the effect of magnetic field on ρ . As it is well known, when a magnetic field is applied on a ferromagnet, the phase transition is suppressed because the magnetization will never tend to zero. Critical fluctuations are reduced, the number of clusters of antiparallel spins diminishes. As a consequence, we expect that the peak of the resistivity will be reduced and disappears at

high fields. This is what we observed in simulations. We show results of ρ for several fields in Fig. 4.

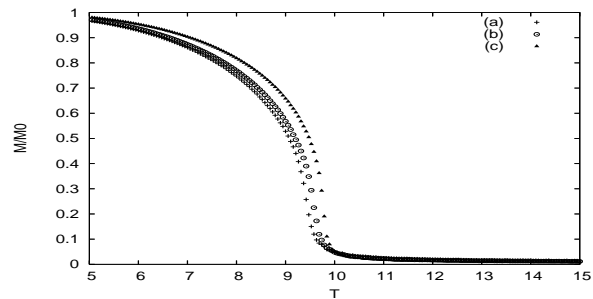


FIG. 2: Lattice magnetization versus temperature T with different thicknesses (N_z) of the film: crosses, void circles and black triangles indicate data for $N_z=5$, 8 and bulk, respectively. $T_c(\text{bulk}) \simeq 9.79$, $T_c(N_z = 8) \simeq 9.58$ and $T_c(N_z = 5) \simeq 9.47$.

B. Effect of surface

The picture suggested above on the physical mechanism causing the variation of the resistivity helps to understand the surface effect shown here. Since the surface spins suffer more fluctuations due to the lack of neighbors, we expect that surface lattice spins will scatter more strongly itinerant spins than the interior lattice spins. The resistivity therefore should be larger near the surface. This is indeed what we observed. The effect however is very small in the case where only a single surface layer is perturbed. To enhance the surface effect, we have perturbed a number of layers near the surface: we considered a sandwich of three films: the middle film of 4 layers is placed between two surface films of 5 layers each. The in-plane interaction between spins of the surface films is taken to be J_s and that of the middle film is J . When $J_s = J$ one has one homogeneous 14-layer film. We have simulated the two cases where $J_s = J$ and $J_s = 0.2J$ for sorting out the surface effect. In the absence of itinerant

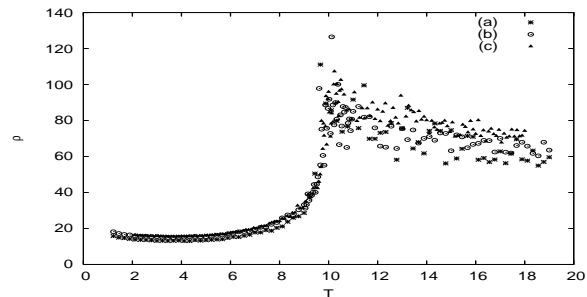


FIG. 3: Resistivity ρ in arbitrary unit versus temperature T for different film thicknesses. Crosses (a), void circles (b) and black triangles (c) indicate data for bulk, $N_z=8$ and 5, respectively.

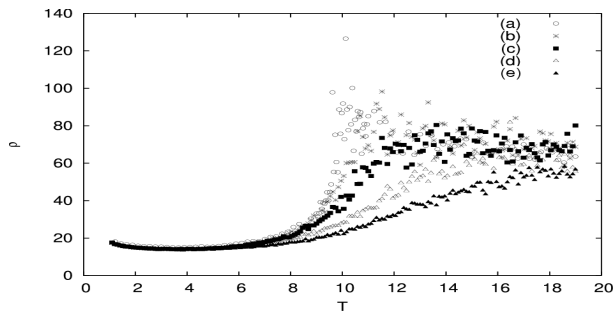


FIG. 4: Resistivity ρ in arbitrary unit versus temperature T , for different magnetic fields. Void circles, stars, black rectangles, void triangles and black triangles indicate, respectively, data for (a) $B = 0$, (b) $B = 0.1J$, (c) $B = 0.3J$, (d) $B = 1J$ and (e) $B = 2J$.

ant spins, the lattice spins undergo a single phase transition at $T_c \simeq 9.75$ for $J_s = J$, and two transitions when $J_s = 0.2J$: the first transition occurs at $T_1 \simeq 4.20$ for "surface" films and the second at $T_2 \simeq 9.60$ for "middle" film. This is seen in Fig. 5 where the magnetization of the surface films drops at T_1 and the magnetization of the middle film remains up to T_2 . The susceptibility has two peaks in the case $J_s = 0.2J$. The resistivity of this case is shown in Fig. 6: at $T < T_1$ the whole system is ordered, ρ is therefore small. When $T_1 \leq T \leq T_2$ the surface spins are disordered while the middle film is still ordered: itinerant spins encounter strong scattering in the two surface films, they "escape", after multiple collisions, to the middle film. This explains the peak of the surface resistivity at T_1 . Note that already far below T_1 , a number of surface itinerant spins begin to escape to the middle film, making the resistivity of the middle film to decrease with increasing T below T_1 up to T_2 , as seen in Fig. 6. Note that there is a small shoulder of the total resistivity at T_1 . In addition, in the range of temperatures between T_1 and T_2 the spins travel almost in the middle film with a large density resulting in a very low resistivity of the middle film. For $T > T_2$, itinerant spins flow in every part of the system.

C. Effect of impurity

In this subsection, we take back $N_x = N_y = 20$ and $N_z = 8$.

1. Magnetic impurities

To treat the case with impurities, we replace randomly a number of lattice spins S by impurity spins $\sigma = 2$. We suppose an RKKY interaction between impurity spins (see Eq. 8). Figure 7 shows the lattice magnetization for several impurity concentrations. We see that critical temperature T_c increases with magnetic impurity's

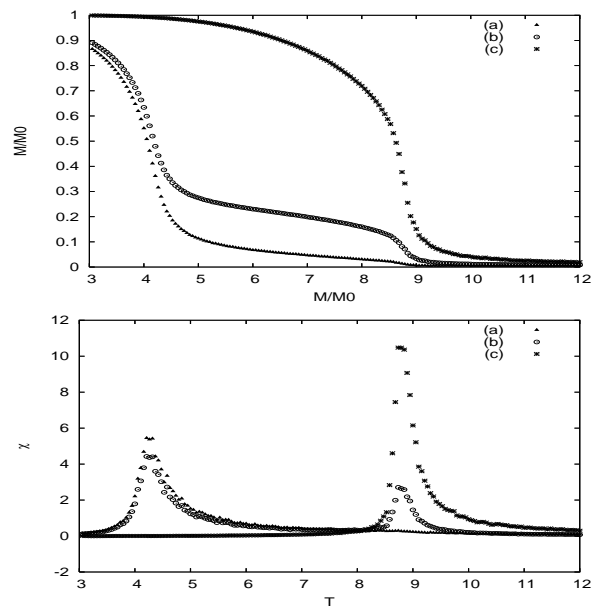


FIG. 5: Upper figure: Magnetization versus T in the case where the system is made of three films: the first and the third have 5 layers with a weaker interaction J_s , while the middle has 4 layers with interaction $J = 1$. We take $J_s = 0.2J$. Black triangles: magnetization of the surface films, stars: magnetization of the middle film, void circles: total magnetization. Lower figure: Susceptibility versus T of the same system as in the upper figure. Black triangles: susceptibility of the surface films, stars: susceptibility of the middle films, void circles: total susceptibility. See text for comments.

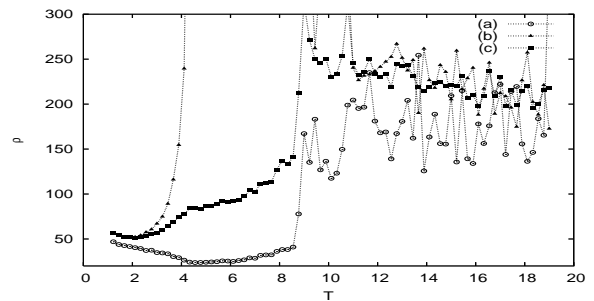


FIG. 6: Resistivity ρ in arbitrary unit versus T of the system described in the previous figure's caption. Black triangles: resistivity of the surface films, void circles: resistivity of the middle film, black squares: total resistivity. See text for comments.

concentration. We understand that large-spin impurities must reinforce the magnetic order.

In Figs. 8, 9 and 10, we compare a system without impurity to systems with respectively 1 and 2 and 5 percents of impurities. The temperature of resistivity's peak is a little higher than the critical temperature and we see that the peak height increases with increasing impurity concentration (see Fig. 10). This is easily explained by the fact that when large-spin impurities are introduced into the system, additional magnetic clusters

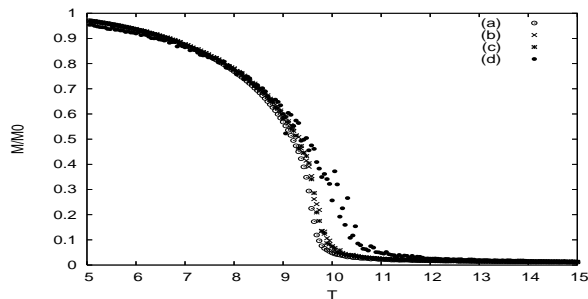


FIG. 7: Lattice magnetization versus temperature T with different concentrations of magnetic impurities C_I . Void circles, crosses, stars and black diamonds indicate, respectively, data for (a) $C_I = 0\%$, (b) $C_I = 1\%$, (c) $C_I = 2\%$ and (d) $C_I = 5\%$.

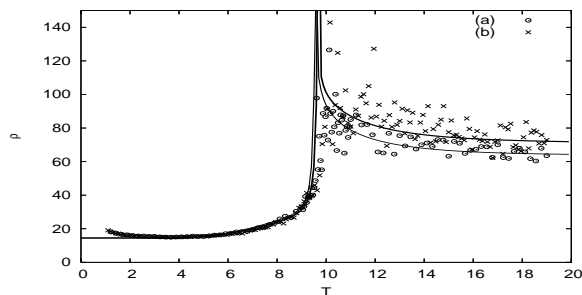


FIG. 8: Resistivity ρ in arbitrary unit versus temperature T . Two cases are shown: without (a) and with 1% (b) of magnetic impurities (void circles and crosses, respectively). Our result using the Boltzmann's equation is shown by the continuous curves (see sect. IV): thin and thick lines are for (a) and (b), respectively. Note that $T_c \simeq 9.68$ for $C_I = 1\%$.

around these impurities are created in both ferromagnetic and paramagnetic phases. They enhance therefore ρ .

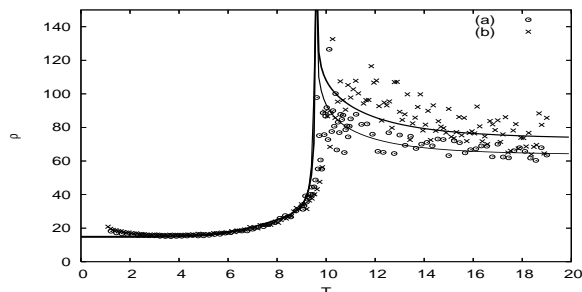


FIG. 9: Resistivity ρ in arbitrary unit versus temperature T . Two cases are shown: without and with 2% of magnetic impurities (void circles and crosses, respectively). Our result using the Boltzmann's equation is shown by the continuous curves (see sect. IV): thin and thick lines are for (a) and (b), respectively. $T_c \simeq 9.63$ for 2% .

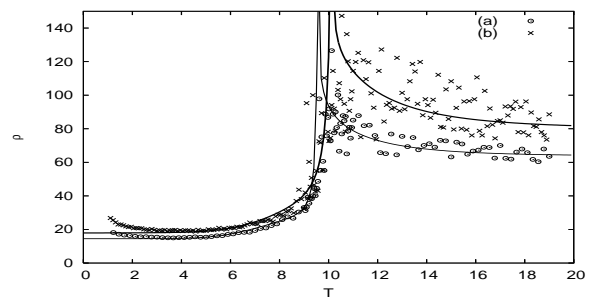


FIG. 10: Resistivity ρ in arbitrary unit versus temperature T . Two cases are shown: without (a) and with 5% of magnetic impurities (b) (void circles and crosses, respectively). Our result using the Boltzmann's equation is shown by the continuous curves (see sect. IV): thin and thick lines are for (a) and (b), respectively. $T_c \simeq 10.21$ for 5%.

2. Non-magnetic impurities

For the case with non-magnetic impurities, we replace randomly a number of lattice spins S by zero-spin impurities $\sigma = 0$. Figures 11, 12 and 13 show, respectively, the lattice magnetizations and the resistivities for non-magnetic impurity concentrations 1% and 5%. We observe that non-magnetic impurities reduce the critical temperature and the temperature of the resistivity's peak. This can be explained by the fact that the now "dilute" lattice spins has a lower critical temperature so that the scattering of itinerant spins by lattice-spin clusters should take place at lower temperatures.

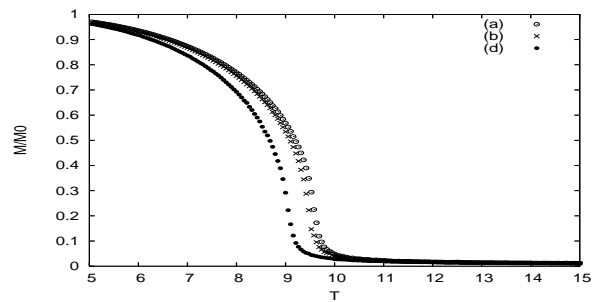


FIG. 11: Lattice magnetization versus temperature T for different concentrations of non-magnetic impurities: (a) $C_I = 0\%$ (void circles), (b) $C_I = 1\%$ (crosses) and (c) $C_I = 5\%$ (black diamonds).

D. Discussion

De Gennes and Friedel¹ have shown that the resistivity ρ is related to the spin correlation $\langle \mathbf{S}_i \cdot \mathbf{S}_j \rangle$. They have suggested therefore that ρ behaves as the magnetic susceptibility χ . However, unlike the susceptibility which diverges at the transition, the resistivity observed in many experiments goes through a finite maximum, i. e. a cusp,

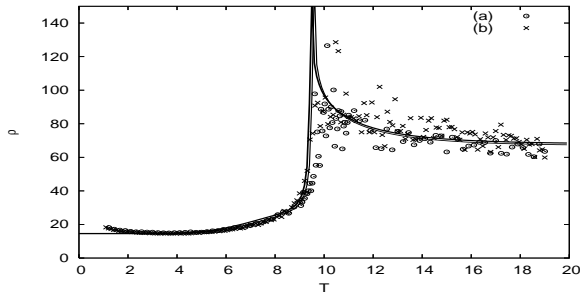


FIG. 12: Resistivity ρ in arbitrary unit versus temperature T for two cases: without (a) and with 1% of non-magnetic impurities (b) (void circles and crosses, respectively). Our result using the Boltzmann's equation is shown by the continuous curves (see sect. IV): thin and thick lines are for (a) and (b), respectively.

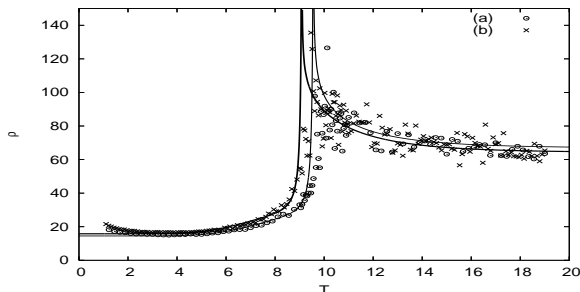


FIG. 13: Resistivity ρ in arbitrary unit versus temperature T for two cases: without (a) and with 5% of non-magnetic impurities (b) (void circles and crosses, respectively). Our result using the Boltzmann's equation is shown by the continuous curves (see sect. IV): thin and thick lines are for (a) and (b), respectively.

without divergence. To explain this, Fisher and Langer¹⁴ and then Kataoka¹⁶ have shown that the cusp is due to short-range correlation. This explanation is in agreement with many experimental data but not all (see Ref. 15 for review on early experiments).

Let us recall that $\langle E \rangle \propto \sum_{i,j} \langle \mathbf{S}_i \cdot \mathbf{S}_j \rangle$ where the sum is taken over NN (or short-range) spin pairs while $T\chi \propto \langle (\sum_i \mathbf{S}_i)^2 \rangle = \sum_{i,j} \langle \mathbf{S}_i \cdot \mathbf{S}_j \rangle$ where the sum is performed over *all* spin pairs. This is the reason why short-range correlation yields internal energy and long-range correlation yields susceptibility.

Roughly speaking, if $\langle \mathbf{S}_i \cdot \mathbf{S}_j \rangle$ is short-ranged, then ρ behaves as $\langle E \rangle$ so that the temperature derivative of the resistivity, namely $d\rho/dT$, should behave as the specific heat with varying T . Recent experiments have found this behavior (see for example Ref. 5).

Now, if $\langle \mathbf{S}_i \cdot \mathbf{S}_j \rangle$ is long-ranged, then ρ behaves as the magnetic susceptibility as suggested by de Gennes and Friedel.¹ In this case, ρ undergoes a divergence at T_c as χ . One should have therefore $d\rho/dT > 0$ at $T < T_c$ and $d\rho/dT < 0$ at $T > T_c$. In some experiments, this has been found in for example in magnetic semiconductors (Ga,Mn)As⁶ (see also Ref. 15 for review on older ex-

periments). We think that all systems are not the same because of the difference in interactions, so one should not discard a priori one of these two scenarios.

In this paper, we suggest another picture to explain the cusp: when T_c is approached, large clusters of up (resp. down) spins are formed in the critical region above T_c . As a result, the resistance is much larger than in the ordered phase: itinerant electrons have to steer around large clusters of opposite spins in order to go through the entire lattice. Thermal fluctuations are not large enough to allow the itinerant spin to overcome the energy barrier created by the opposite orientation of the clusters in this temperature region. Of course, far above T_c , most clusters have a small size, the resistivity is still quite large with respect to the low- T phase. However, ρ decreases as T is increased because thermal fluctuations are more and more stronger to help the itinerant spin to overcome energy barriers.

What we have found here is a peak of ρ , not a peak of $d\rho/dT$. So, our resistivity behaves as the susceptibility although the peak observed here is not sharp and no divergence is observed. We believe however that, similar to commonly known disordered systems, the susceptibility peak is broadened more or less because of the disorder. The disorder in the system studied here is due the lack of periodicity in the positions of moving itinerant spins.

IV. SEMI-NUMERICAL THEORY

In this paragraph, we show a theory based on the Boltzmann's equation in the relaxation-time approximation. To solve completely this equation, we shall need some numerical data from MC simulations for the cluster sizes as will be seen below. Using these data, we show that our MC result of resistivity is in a good agreement with this theory.

Let us formulate now the Boltzmann's equation for our system. When we think about the magnetic resistivity, we think of the interaction between lattice spins and itinerant spins. We recognize immediately the important role of the spin-spin correlation function in the determination of the mean free-path. If we inject through the system a flow of spins "polarized" in one direction, namely "up", we can consider clusters of "down" spins in the lattice as "defect clusters", or as "magnetic impurities", which play the role of scattering centers. We therefore reduce the problem to the determination of the number and the size of defect clusters. For our purpose, we use the Boltzmann's equation with uniform electric field but without gradient of temperature and gradient of chemical potential. We write the equation for f , the Fermi-Dirac distribution function of itinerant electrons, as

$$\left(\frac{\hbar\mathbf{k}\cdot e\mathbf{E}}{m}\right)\left(\frac{\partial f^0}{\partial \varepsilon}\right) = \left(\frac{\partial f}{\partial t}\right)_{coll}, \quad (11)$$

where \mathbf{k} is the wave vector, e and m the electronic charge

and mass, ϵ the electron energy. We use the following relaxation-time approximation

$$\left(\frac{\partial f_k}{\partial t}\right)_{coll} = -\left(\frac{f_k^1}{\tau_k}\right), \quad f_k^1 = f_k - f_k^0, \quad (12)$$

where τ_k is the relaxation time. Supposing elastic collisions, i. e. $k = k'$, and using the detailed balance we have

$$\left(\frac{\partial f_k}{\partial t}\right)_{coll} = \frac{\Omega}{(2\pi)^3} \int w_{k',k}(f_{k'}^1 - f_k^1) dk', \quad (13)$$

where Ω is the system volume, $w_{k',k}$ the transition probability between k and k' . We find with Eq. (12) and Eq. (13) the following well-known expression

$$\left(\frac{1}{\tau_k}\right) = \frac{\Omega}{(2\pi)^3} \int w_{k',k}(1 - \cos \theta) \times \sin \theta k'^2 dk' d\theta d\phi, \quad (14)$$

where θ and ϕ are the angles formed by \mathbf{k}' with \mathbf{k} , i. e. spherical coordinates with z axis parallel to \mathbf{k} .

We use now for Eq. (14) the "Fermi golden rule" and we obtain

$$\left(\frac{1}{\tau_k}\right) = \frac{\Omega m}{\hbar^3 2\pi k} \int |\langle k'|V|k \rangle|^2 (1 - \cos \theta) \sin \theta \times \delta(k' - k) k'^2 dk' d\theta \quad (15)$$

We give for the potential V the following expression which reminds the form of the interactions (4)-(5)

$$V = V_0 \exp\left(\frac{-r}{\xi(T)}\right), \quad (16)$$

where $\xi(T)$ is the size of the defect cluster and V_0 a constant. We resolve Eq. (15) with Eq. (16) and we have the following expression

$$\left(\frac{1}{\tau_k}\right) = \left(\frac{32V_0^2 \Omega m k \pi}{\hbar^3}\right) \int \frac{\sin \theta (1 - \cos \theta)}{(K^2 + \xi^{-2})^3} d\theta, \quad (17)$$

where $K = |\vec{k} - \vec{k}'|$ is given by

$$K = |\vec{k} - \vec{k}'| = k[2(1 - \cos \theta)]^{1/2}, \quad (18)$$

Integrating Eq. (17) we obtain

$$\left(\frac{1}{\tau_k}\right) = \frac{32(V_0 \Omega)^2 m \pi}{(2k\hbar)^3} n_c \xi^2 \times \left[1 - \frac{1}{1 + 4k^2 \xi^2} - \frac{4k^2 \xi^2}{(1 + 4k^2 \xi^2)^2}\right] \quad (19)$$

where n_c is the number of clusters of size ξ . We integrate Eq. (19) for the interval $[0, k_F]$ and we obtain finally

$$\left(\frac{1}{\tau}\right) = \frac{(4V_0 \Omega m)^2}{\pi(\hbar)^{3/2}} n_c \xi^2 \times \left[\frac{1}{1 + (2k_F \xi)^2} + \ln(1 + (2k_F \xi)^2) - 1\right] \quad (20)$$

Note that although the relaxation time τ is averaged over all states in the Fermi sphere, i. e. states at $T = 0$, its temperature dependence comes from the parameters ξ and n_c . These will be numerically determined in the following. If we know τ we can calculate the resistivity by the Drude expression

$$\rho_m = \frac{m}{ne^2} \frac{1}{\tau}, \quad (21)$$

Let us use now the Hoshen-Kopelman's algorithm¹⁹ to determine the mean value of ξ and the number of the cluster's mean size, for different temperatures. The Hoshen-Kopelman's algorithm allows to regroup into clusters spins with equivalent value for $T < T_c$ or equivalent energy for $T > T_c$. Using this algorithm during our MC simulation at a given T , we obtain a "histogram" representing the number of clusters as a function of the cluster size. For temperature T below T_c , we call a cluster a group of parallel spins surrounded by opposite spins, and for T above T_c a cluster is a group of spins with the same energy. At a given T , we estimate the average size ξ using the histogram as follows: calling N_i the number of spins in the cluster and P_i the probability of the cluster deduced from the histogram, we have

$$\xi = \frac{\sum_i N_i P_i}{\sum_i P_i}, \quad (22)$$

In doing this we obtain ξ for the whole temperature range. We note that we can fit the cluster size ξ with the following formula

$$\xi = A|T_c - T|^{\nu/3}, \quad (23)$$

where ν is a fitting parameter and A a constant. These parameters are different for $T < T_c$ and $T > T_c$. Figure 14 and Figure 15 show the average size and the average number of cluster versus temperature. To simplify our approach we consider that the cluster's geometry is a sphere with radius ξ . Note that due to the fact that our fitting was made separately for $T < T_c$ and $T > T_c$, no effort has been made for the matching at $T = T_c$ exactly, but this does not affect the behavior discussed below.

We distinguish hereafter temperatures below and above T_c in establishing our theory. We write

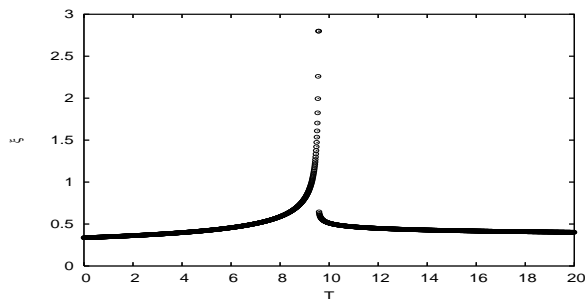
$$T < T_c \left[\begin{array}{l} \rho_m = \rho_0 \left(1 + C_{inf} n_c \xi^2 \left[-1 + \frac{1}{1 + (2k_F \xi)^2} + \ln(1 + (2k_F \xi)^2)\right]\right), \\ \xi = \left(\frac{3A_{inf}}{16\pi}\right)^{1/3} (T_c - T)^{\nu_{inf}/3}, \\ n_c = \left(\frac{B_{inf}}{2\alpha\pi}\right) \times \exp\left[\frac{-(T - T_G)^2}{2\alpha^2}\right]. \end{array} \right. \quad (24)$$

TABLE I: Various numerical values obtained by MC simulations which are used to plot Eqs. (24) and (25).

Impurity		T_c	T_G	ν_{inf}	ν_{sup}	α
0%	S=1	9.58	7.4443 +/- 0.066	-0.9254 +/- 0.015	-0.2267 +/- 0.006	1.51875 +/- 0.07
1%	$\sigma=2$	9.68	7.5006 +/- 0.054	-0.9253 +/- 0.017	-0.1449 +/- 0.006	1.62908 +/- 0.06
2%	$\sigma=2$	9.63	7.7103 +/- 0.049	-0.9856 +/- 0.016	-0.1135 +/- 0.004	1.64786 +/- 0.05
5%	$\sigma=2$	10.2	7.9658 +/- 0.094	-1.1069 +/- 0.016	-0.0747 +/- 0.002	2.13618 +/- 0.10
1%	$\sigma=0$	9.47	7.2866 +/- 0.062	-0.9028 +/- 0.013	-0.2106 +/- 0.006	1.51766 +/- 0.06
5%	$\sigma=0$	9.10	7.0105 +/- 0.054	-0.9381 +/- 0.015	-0.1607 +/- 0.006	1.47261 +/- 0.05

$$T > T_c \left[\begin{aligned} \rho_m &= \rho_\infty \left(1 + C_{sup} n_c \xi^2 \left[-1 + \frac{1}{1 + (2k_F \xi)^2} \right. \right. \right. \\ &\quad \left. \left. \left. + \ln(1 + (2k_F \xi)^2) \right] \right), \\ \xi &= \left(\frac{3A_{sup}}{16\pi} \right)^{1/3} (T - T_c)^{\nu_{sup}/3}, \\ n_c &= B_{sup} \exp[-D(T - T_c)] + n_0. \end{aligned} \right. \quad (25)$$

In Eq. (24) we call T_G the temperature on which the cluster of small size are gathering to form bigger cluster. This temperature marks the limit when one enters

FIG. 14: Mean size ξ of magnetic clusters versus temperature T for both above and below T_c .

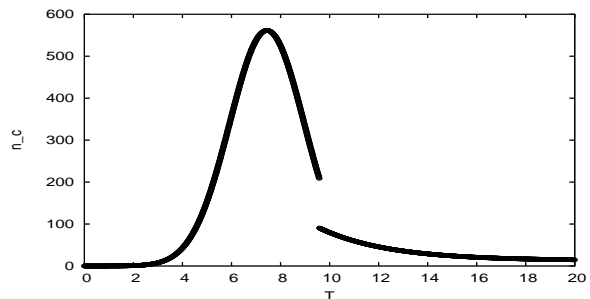
Based on those results, we can extract the resistivity ρ_I corresponding only to the addition of impurities. ρ_I is defined as

$$\rho_I = \rho_m - \rho_{standard}, \quad (26)$$

where $\rho_{standard}$ is the resistivity without impurities (see the first line of Table 1). We compare now the resistivity ρ_I with experiments realized by Shwerner and Cuddy.³ It is important to note that the change of behavior can be explained if we use the correct value for ν , T_c , T_G , etc. Figure 16 shows ρ_I with magnetic impurities corresponding to the Ni-Fe system, while Fig. 17 shows ρ_I in the case of non-magnetic impurities corresponding to the Ni-Cr case.

the critical region from below. In Eq. (24), α is the half-width of the peak of n_c shown in Fig. 15. ρ_0 is the resistivity at $T = 0$ and ρ_∞ is that at $T = \infty$.

We summarize in Table 1 the different results obtained for the cases studied by MC simulations shown above. Other parameters A_{inf} , B_{inf} , C_{inf} , A_{sup} , B_{sup} and C_{sup} are fitting parameters which are not of physical importance and therefore not given here for the sake of clarity. Using the numerical values of Table 1 and the average cluster size and cluster number shown in Fig. 14 and Fig. 15, we plot Eqs. (24) and (25) by continuous lines in Figs. 8-13 to compare with MC simulations shown in these figures. We emphasize that our theory provides a good "fit" for simulation results.

FIG. 15: Number of average cluster size n_c for both above and below T_c .

We see that the form of ρ_I of the alloys Ni-Fe(1%) and Ni-Fe(0.5%) experimentally observed³ can be compared to the curves of 1% and 2% of magnetic impurities shown in Fig. 16. For Ni-Cr(1%) and Ni-Cr(2%), experimental curves are in agreement with our results of non-magnetic impurities shown in Fig. 17.

Finally, to close this section, let us show theoretically from the equations obtained above, the effects of the density of itinerant spins on the resistivity. Figure 18 shows that, as the density n_0 is increased, the peak of ρ diminishes. It is noted that this behavior is very similar with that obtained by Kataoka.¹⁶ In our MC simulation shown above, we have chosen $n_0 = 1/4$. Such a weak density has allowed us to avoid the flip of lattice spins upon interac-

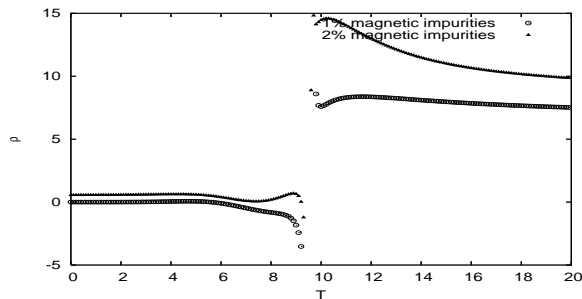


FIG. 16: Resistivity ρ_I in arbitrary unit versus temperature T . Void circles and black triangles indicate data for 1% and 2% magnetic impurities, respectively.

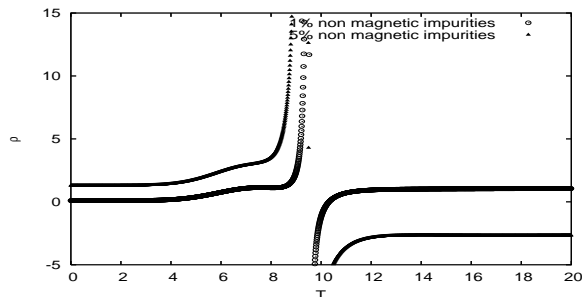


FIG. 17: Resistivity ρ_I in arbitrary unit versus temperature T . Void circles and black triangles indicate data for 1% and 5% non magnetic impurities, respectively.

tion with itinerant spins. In the case of strong density, we expect that a number of lattice spins, when surrounded by a large number of itinerant spins, should flip to accommodate themselves with their moving neighbors. So the lattice ordering should be affected. As a consequence, critical fluctuations of lattice spins are more or less suppressed, so is the peak's height, just like in the case of an applied magnetic field. Kataoka¹⁶ has found this in his calculation by taking into account the spin flipping: the resistivity's peak disappears then at the transition. It would be interesting to perform more MC simulations with varying n_0 . This is left for a future investigation.

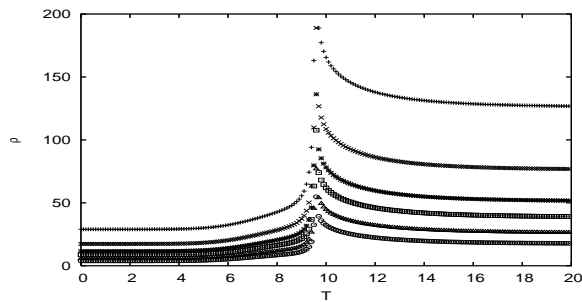


FIG. 18: Resistivity ρ in arbitrary unit versus temperature T for different densities of itinerant spins. Curves from top to bottom are for $n_0 = 0.2, 0.33, 0.5, 0.7, 1$ and 1.5 .

V. CONCLUSION

We have shown in this paper results of MC simulations on the transport of itinerant spins interacting with localized lattice spins in a ferromagnetic FCC thin film. Various interactions have been taken into account. We found that the spin current is strongly dependent on the lattice spin ordering: at low T itinerant spins whose direction is parallel to the lattice spins yield a strong current, namely a small resistivity. At the ferromagnetic transition, the resistivity undergoes a huge peak. At higher temperatures, the lattice spins are disordered, the resistivity is still large but it decreases with increasing T . From the discussion given in subsection III D, we conclude that the resistivity ρ of the model studied here behaves as the magnetic susceptibility with a peak at T_c . $d\rho/dT$, differential resistivity is thus negative for $T > T_c$. The peak of the resistivity obtained here is in agreement with experiments on magnetic semiconductors (Ga,Mn)As for example.⁶ Of course, to compare the peak's shape experimentally obtained for each material, we need to refine our model parameters for each of them. This was not the purpose of the present paper. Instead, we were looking for generic effects to show physical mechanisms lying behind the temperature dependence of the spin resistivity. In this spirit, we note that early theories have related the origin of the peak to the spin-spin correlation, while our interpretation here is based on the existence of defect clusters formed in the critical region. This interpretation has been verified by calculating the number and the size of clusters as a function of T by the use of Hoshen-Kopelman's algorithm. We have formulated a theory based on the Boltzmann's equation. We solved this equation using numerical data obtained for the number and the size of average cluster at each T . The results on the resistivity are in a good agreement with MC results.

Finally, let us conclude by saying that the clear physical picture we provide in this paper for the understanding of the behavior of the resistivity in a single ferromagnetic film will help to understand properties of resistivity in more complicated systems such as antiferromagnets, non-Ising spin systems, frustrated spin systems, disordered media, ... where much has to be done.

-
- ¹ P.-G. de Gennes and J. Friedel, *J. Phys. Chem. Solids* **4**, 71 (1958).
- ² A. Fert and I. A. Campbell, *Phys. Rev. Lett.* **21**, 1190 (1968); I. A. Campbell, *Phys. Rev. Lett.* **24**, 269 (1970).
- ³ F. C. Shwerer and L. J. Cuddy, *Phys. Rev.* **2**, 1575 (1970).
- ⁴ Alla E. Petrova, E. D. Bauer, Vladimir Krasnorussky, and Sergei M. Stishov, *Phys. Rev. B* **74**, 092401 (2006).
- ⁵ S. M. Stishov, A.E. Petrova, S. Khasanov, G. Kh. Panova, A.A.Shikov, J. C. Lashley, D. Wu, and T. A. Lograsso, *Phys. Rev. B* **76**, 052405 (2007).
- ⁶ F. Matsukura, H. Ohno, A. Shen and Y. Sugawara, *Phys. Rev. B* **57**, R2037 (1998).
- ⁷ M. N. Baibich, J. M. Broto, A. Fert, F. Nguyen Van Dau, F. Petroff, P. Etienne, G. Creuzet, A. Friederich and J. Chazelas, *Phys. Rev. Lett.* **61**, 2472 (1988).
- ⁸ P. Grunberg, R. Schreiber, Y. Pang, M. B. Brodsky and H. Sowers, *Phys. Rev. Lett.* **57**, 2442 (1986); G. Binash, P. grunberg, F. Saurenbach and W. Zinn, *Phys. Rev. B* **39**, 4828 (1989).
- ⁹ A. Barthélémy, A. Fert, J.-P. Contour and M. Bowen, *J. Mag. Mag. Mater.* **242-245**, 68 (2002).
- ¹⁰ See review by E. Y. Tsybal and D. G. Pettifor, *Solid State Physics*, Academic Press (San Diego), Vol. 56, pp. 113-237 (2001).
- ¹¹ See review on Semiconductor Spintronics by T. Dietl, in *Lectures Notes*, vol. 712, Springer (Berlin), pp. 1-46 (2007).
- ¹² See review on Oxide Spintronics by Manuel Bibes and Agn Barthy, in a Special Issue of *IEEE Transactions on Electron Devices on Spintronics*, *IEEE Trans. Electron. Devices* **54**, 1003 (2007).
- ¹³ Paul P. Craig, Walter I. Goldberg, T. A. Kitchens and J. I. Budnick, *Phys. Rev. Lett.* **19**, 1334 (1967).
- ¹⁴ M. E. Fisher and J.S. Langer, *Phys. Rev. Lett.* **20**, 665 (1968).
- ¹⁵ S. Alexander, J. S. Helman and I. Balberg, *Phys. Rev. B.* **13**, 304 (1975).
- ¹⁶ Mitsuo Kataoka, *Phys. Rev. B* **63**, 134435-1 (2001).
- ¹⁷ K. Akabli, H. T. Diep and S. Reynal, *J. Phys.: Condens. Matter* **19**, 356204 (2007).
- ¹⁸ R. Brucas and M. Hanson; *J. Magn. Magn. Mater.* **310**, 2521 (2007).
- ¹⁹ J. Hoshen and R. Kopelman, *Phys. Rev. B* **14**, 3438 (1974).
- ²⁰ K. Binder and D. W. Heermann, *Monte Carlo Simulation in Statistical Physics*, Springer, New York (2002).